

Tsunami Simulations for Regional Sources in the South China and Adjoining Seas

EMILE A. OKAL,¹ COSTAS E. SYNOLAKIS,^{2,3,4} and NIKOS KALLIGERIS^{3,4}

Abstract—We present 14 scenarios of potential tsunamis in the South China Sea and its adjoining basins, the Sulu and Sulawesi Seas. The sources consist of earthquake dislocations inspired by the study of historical events, either recorded (since 1900) or described in historical documents going back to 1604. We consider worst-case scenarios, where the size of the earthquake is not limited by the largest known event, but merely by the dimension of the basin over which a coherent fault may propagate. While such scenarios are arguably improbable, they may not be impossible, and as such must be examined. For each scenario, we present a simulation of the tsunami's propagation in the marine basin, exclusive of its interaction with the coastline. Our results show that the South China, Sulu and Sulawesi Seas make up three largely independent basins where tsunamis generated in one basin do not leak into another. Similarly, the Sunda arc provides an efficient barrier to tsunamis originating in the Indian Ocean. Furthermore, the shallow continental shelves in the Java Sea, the Gulf of Thailand and the western part of the South China Sea significantly dampen the amplitude of the waves. The eastern shores of the Malay Peninsula are threatened only by the greatest—and most improbable—of our sources, a mega-earthquake rupturing all of the Luzon Trench. We also consider two models of underwater landslides (which can be triggered by smaller events, even in an intraplate setting). These sources, for which there is both historical and geological evidence, could pose a significant threat to all shorelines in the region, including the Malay Peninsula.

Key words: Tsunami, South China Sea, focal mechanism, numerical simulation.

1. Introduction

We consider in this study a number of tsunami scenarios in the South China Sea and its adjoining

basins. As shown in Fig. 1, the South China Sea constitutes an essentially enclosed basin, which communicates with the Indian and Pacific Oceans only through a number of narrow straits whose widths vary from 250 km (Luzon Straits) to only a few km (Malacca Straits). In addition, the island of Borneo is separated from the Philippines by the Sulu and Sulawesi Seas, and from Java and the other Sunda arc islands by the Java Sea, which themselves are basically enclosed basins. We do not include in the present study the Flores, Banda, and Molucca Seas. The geological nature of the South China and adjoining seas is variable, as the eastern half of the South China Sea and the Sulu and Sulawesi Seas are oceanic basins with depths in excess of 4,000 m, while the western South China Sea and the Java Sea are continental shelves not exceeding 200 m in depth.

This region is bordered by some of the most active subduction systems on Earth, notably the Sumatra and Java arcs to the west and south. To the east, the boundary with the Philippine plate is broken up along a number of segments involving the Taiwan, Luzon, East Philippine, Moro, Sangihe and Mindanao subduction zones. As HAMILTON (1979) summarized in a landmark contribution, the extreme complexity of this tectonic pattern is a result of the ongoing collision between the Australian plate to the south and Eurasia to the north, with the added influence of the eastward push of the Chinese block into the Pacific, due to the Himalayan collision.

In this context, and in the wake of the 2004 Sumatra–Andaman disaster, it is important to assess the tsunami hazard which may threaten the South China Sea and its adjoining basins, especially since its shores host a number of mega-cities, as shown in Fig. 1. Our approach in the present paper follows in the general steps of a previous contribution in which we had modeled a number of scenarios for far-field

¹ Department of Earth and Planetary Sciences, Northwestern University, Evanston, IL 60201, USA. E-mail: emile@earth.northwestern.edu

² Department of Civil Engineering, University of Southern California, Los Angeles, CA 90089, USA.

³ Department of Environmental Engineering, Technical University of Crete, 73100 Chania, Greece.

⁴ Institute of Applied and Computational Mathematics, P.O. Box 1385, 71110 Heraklion, Greece.

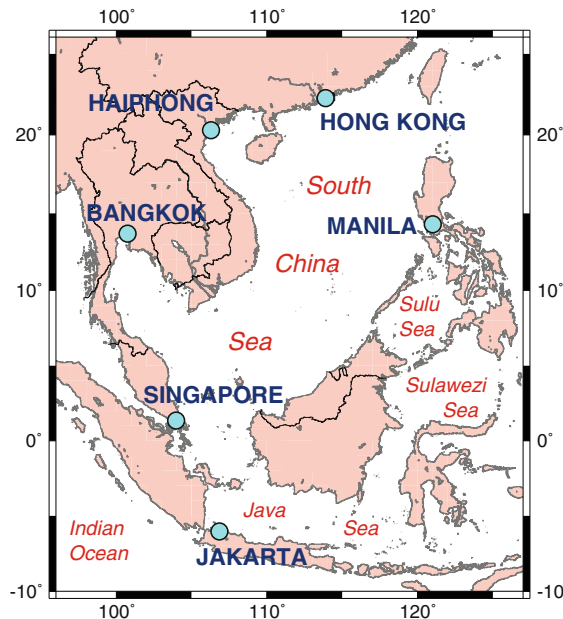


Figure 1

Location map of the study area. The South China Sea and its adjoining basins are labeled, as are some of the major ports located on shores facing their respective basins, or immediately up relevant estuaries

tsunami risk in the Indian Ocean (OKAL and SYNOLAKIS, 2008; hereafter Paper I), and whose general methodology we will follow. In particular, we will consider worst-case scenarios for each of the seismic regions with the potential of generating a tsunami in the South China Sea; however, the emphasis will be on regional sources, since we will show in Sect. 7 that tsunamis originating outside of the basins cannot substantially penetrate them. In addition, we will discuss a few scenarios of landslide-generated tsunamis.

2. Methodology

Figure 2 shows a map of background shallow seismicity in the study area, with individual dots showing earthquakes from the instrumental era (post-1900) for which at least one published magnitude exceeds 7.5. Also shown, as triangles, are pre-instrumental earthquakes documented to have generated locally damaging tsunamis. This map can be used to identify seismic zones where earthquakes

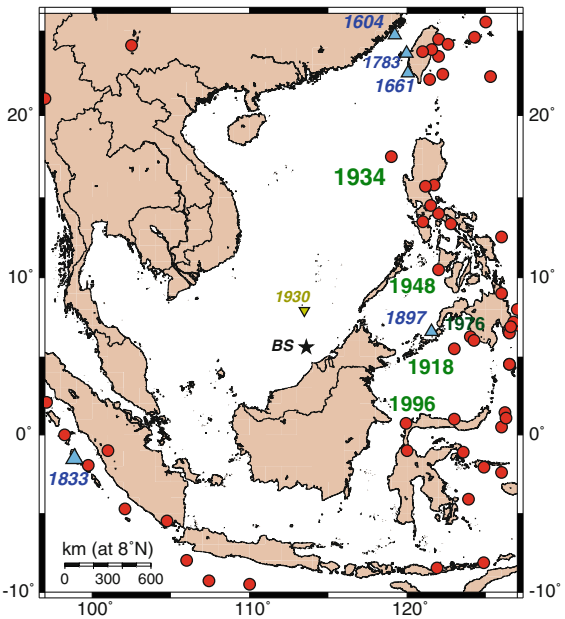


Figure 2

Background seismicity of the study area. The dots denote earthquakes from the instrumented era (1900–2007) with at least one magnitude $M \geq 7.5$; events discussed in the text are labeled in **bold**. Upward triangles (with date in *italics*) identify pre-instrumental earthquakes with a tsunami reported as damaging, and used as a potential scenario in the text. The star identifies the Brunei Slide (BS) discussed in Sect. 8, and the inverted triangle the nearby intraplate earthquake of 21 July 1930

could generate tsunamis potentially damaging in the South China Sea.

In each of these regions, and following the approach in Paper I, we examine documented earthquakes having generated tsunamis and, when necessary, conduct a full seismological study of their source based on historical seismograms. We then discuss whether larger events could take place along similar fault systems. We are motivated in this respect by the documented variability of the mode of strain release along a regional plate boundary. In lay language, even large events along a given subduction zone are not necessarily repeats of each other; they can vary in size, and the last (and obviously best-documented) large earthquake may not represent the potential maximum event along the boundary. This point was first illustrated by ANDO (1975) in the case of the Nankai Trough, and similar conclusions were reached in a growing number of provinces, e.g., central Chile (CISTERNAS *et al.*, 2005), southern Peru

Table 1
Parameters of dislocation sources used in this study

Number of scenario	Description	Figure	Moment M_0 (10^{28} dyn cm)	Length L (km)	Width W (km)	Slip Δu (m)	Focal mechanism			Depth to top of fault (km)
							ϕ (°)	δ (°)	λ (°)	
1	Mindanao 1976	Fig. 3	1.9	150	75	3.5	327	22	69	10
2	Mindanao 1918	Fig. 5	3.0	200	75	4.1	327	22	69	10
3	Sulawesi 1996	Fig. 6	0.8	90	60	3.0	53	7	66	10
4	Hypothetical North Sulawesi	Fig. 7	4.4	250	70	5	100	20	93	10
5	Sulu Islands 1897	Fig. 8	4.5	300	60	5	45	30	90	10
5a	Sulu Islands variant		10	500	60	7	45	30	90	10
6	Hypothetical West of Panay	Fig. 9	1.5	120	60	3.5	349	12	83	10
7a	West of Luzon 1934	Fig. 11	0.22	67	33	2	338	46	53	10
8	Hypothetical Luzon Straits	Fig. 12	10	400	90	6	355	35	57	10
9	Hypothetical Luzon Trench	Fig. 13	10	400	90	6	355	24	72	10
10	Taiwan Straits inspired by 1604	Fig. 14	1.0	111	56	4.5	50	45	90	10
11	Taiwan Straits inspired by 1782	Fig. 15	1.0	111	56	4.5	50	45	90	10
12	Taiwan Straits inspired by 1661	Fig. 16	1.5	127	63	5.1	107	59	-73	10
13	Hypothetical South of Java	Fig. 17	36	500	150	10	290	10	102	10

(OKAL *et al.*, 2006), southern Kuriles (NANAYAMA *et al.*, 2003) and Cascadia (NELSON *et al.*, 2006). In practice, this means that the size of a potential earthquake along a given subduction zone could be limited only by the length along which a coherent rupture could take place.

Once we obtain a model of a potential earthquake, we proceed to simulate the tsunami in the regional field by first using scaling laws (GELLER, 1976) to derive values of the earthquake source parameters (fault length L , fault width W and seismic slip Δu ; see Table 1), which allow the computation of the static field of surface vertical displacement in the source area, using the algorithm of MANSINHA and SMYLINE (1971)). In turn, this field of displacement is taken as the initial wave height of the tsunami, $\eta(x, y; t = 0_+)$, with the additional condition of zero initial velocity. The validity of this classical approximation stems from the generally short nature of the source of an earthquake-generated tsunami, the velocity of rupture along the fault being always hypersonic with respect to the phase velocity of the tsunami. The simulation then proceeds using the MOST code (TRIROV and SYNOLAKIS, 1998; SYNOLAKIS, 2003), which solves the non-linear shallow water approximation of the equations of hydrodynamics using a finite difference algorithm and the method of fractional steps (GODUNOV, 1959). The MOST code has been validated and verified as outlined by SYNOLAKIS *et al.* (2008). The

computation is carried out on a 4-min grid extending from 10°S to 26°N, and from 95°E to 127°E. We do not simulate the interaction of the wave with initially dry land, and the computation is thus stopped at the last marine point in the grid in front of each coastline. The detailed simulation of run-up at individual locations would require a much finer resolution of bathymetry and topography and is beyond the scope of the present paper. Our results are interpreted using maps of the maximum value over time of the wave height $\eta(x, y)$ at each point in the basins.

3. The Sea of Sulawesi

3.1. Scenario 1: The 1976 Mindanao Earthquake

The Mindanao earthquake and tsunami of 16 August 1976 was one of the most devastating events of the twentieth century in the Philippines, and involved subduction of the floor of the Sulawesi Sea under the Island of Mindanao. A detailed seismological study was published by STEWART and COHN (1979) who proposed a moment $M_0 = 1.9 \times 10^{28}$ dyn cm. EKSTRÖM and NETTLES (1997) later obtained a CMT solution based on a restricted digital dataset, with a significantly lower moment (1.1×10^{28} dyn cm). A detailed field survey was carried out by WALLACE *et al.* (1977) who reported run-up

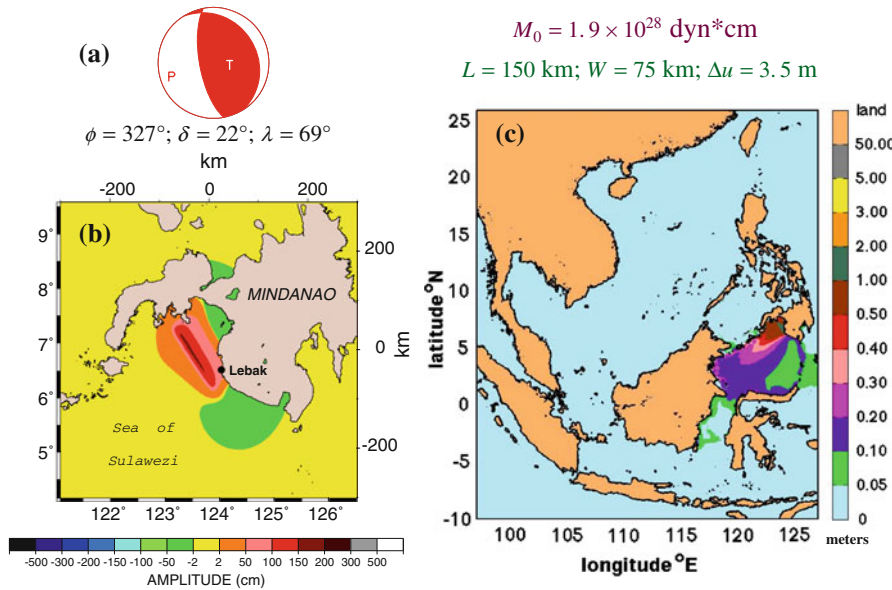


Figure 3
Simulation of *Scenario 1* (Mindanao 1976). **a** Focal mechanism used in simulation. **b** Field of initial displacements computed from MANSINHA and SMYLIE's (1971) algorithm and used as the initial condition of the hydrodynamic simulation. **c** Maximum simulated wave height reached in the study area. Note that the tsunami is essentially contained in the Sea of Sulawesi

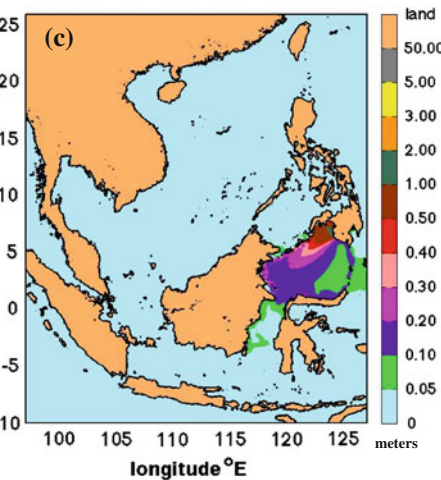
reaching 5 m; the death toll was estimated as high as 8,000, with most casualties reportedly due to the tsunami (SOLOV'EV *et al.*, 1986), making the event the second deadliest tsunami worldwide in the twentieth century.

For the purpose of simulation, we use STEWART and COHN's (1979) model, since the dataset used for the CMT solution was fragmentary. All relevant parameters are listed in Table 1. Figure 3 regroups the static displacement field used as the initial condition of the simulation and the field of maximum wave amplitude computed over the whole basin. The maximum amplitudes (about 1.5 m before run-up on the beaches) are found on the eastern side of the Gulf of Moro and generally compatible with reports of maximum run-up in the area of Lebak (SOLOV'EV *et al.*, 1986). Furthermore, our results show that the tsunami remains essentially contained inside the Sea of Sulawesi, with only minimal penetration of the straits of Makassar to the southwest and of Talaud to the east.

3.2. Scenario 2: The 1918 Mindanao Earthquake

The Moro subduction system, along which the 1976 earthquake took place, was also the site of a

$M_0 = 1.9 \times 10^{28}$ dyn*cm
 $L = 150$ km; $W = 75$ km; $\Delta u = 3.5$ m



major event on 15 August 1918, for which data is obviously more scant. This earthquake was given magnitudes of $M = 8\frac{1}{4}$ by GUTENBERG and RICHTER (1954) and $M_s = 8.0$ by GELLER and KANAMORI (1977). It generated a devastating tsunami whose run-up reached 8 m along the southwestern coast of Mindanao (MASÓ, 1918), even though a definitive death toll was never compiled. As compared with the 1976 event, field descriptions suggest a more powerful tsunami, and a greater impact farther to the southeast along the southwestern coast of Mindanao (SOLOV'EV and GO, 1984). This would indicate that the seismic source of the 1918 event was stronger than in 1976, and in turn that the latter does not represent a worst case scenario along the relevant subduction zone.

In this framework, we conducted a separate seismological study of the 1918 event. Using 26 travel times listed in the International Seismological Summary (ISS), and the algorithm of WYSESSION *et al.* (1991), we relocated the event at 5.58°N, 123.63°E (Fig. 4). This solution is in excellent agreement with STEWART and COHN's (1979) (5.7°N; 123.5°E), even though we keep in our dataset stations with larger residuals. We estimate the quality of our solution by a

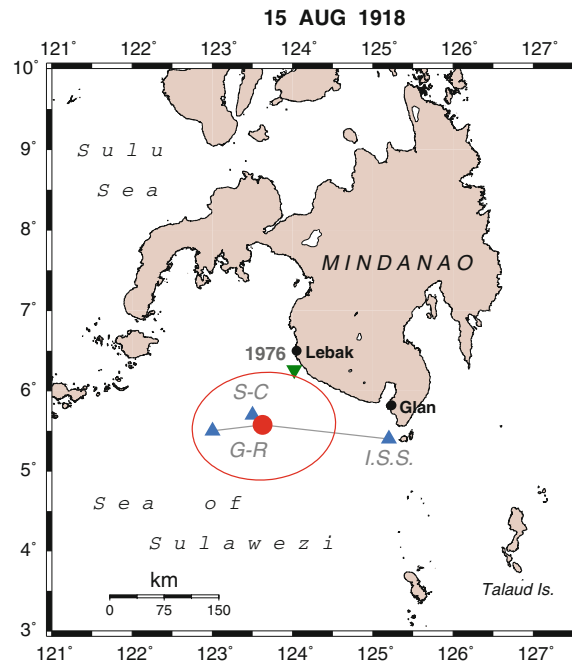


Figure 4

Relocation of the 1918 Mindanao earthquake. The dot is our relocated epicenter with Monte Carlo ellipse ($\sigma_G = 10$ s), the triangles are epicenters proposed by the ISS, GUTENBERG and RICHTER (1954) (G-R) and STEWART and COHN (1979) (S-C), respectively. For reference, the inverted triangle shows the 1976 epicenter

Monte Carlo procedure injecting Gaussian noise with $\sigma_G = 10$ s, adequate for the 1910s. Our confidence ellipse is much larger than the precision of 15 km claimed by STEWART and COHN (1979); it does encompass GUTENBERG and RICHTER's (1954) epicenter, but the ISS epicenter, more than 150 km to the east, is incompatible. The conclusion of this relocation is that the 1918 earthquake originated in the general same section of the Moro subduction system as the 1976 event.

We were further able to assess the moment of the 1918 earthquake from a record of its Love wave at Riverview, Australia (RIV). Assuming the same focal geometry as in 1976, we obtain an average of $M_0 = 3 \times 10^{28}$ dyn cm in the 64–256 s period range. This suggests that the 1918 event was indeed somewhat larger than the 1976 shock, and that the apparently stronger tsunami damage in 1918 in the southern section of coastline, between Lebak and Glan, could reflect a fault line extending farther to the southeast than in 1976.

In this context, we model the 1918 earthquake using a longer fault ($L = 200$ km), and greater slip ($\Delta u = 4.1$ m) than in 1976. Results, shown in Fig. 5, show once again that the tsunami remains contained

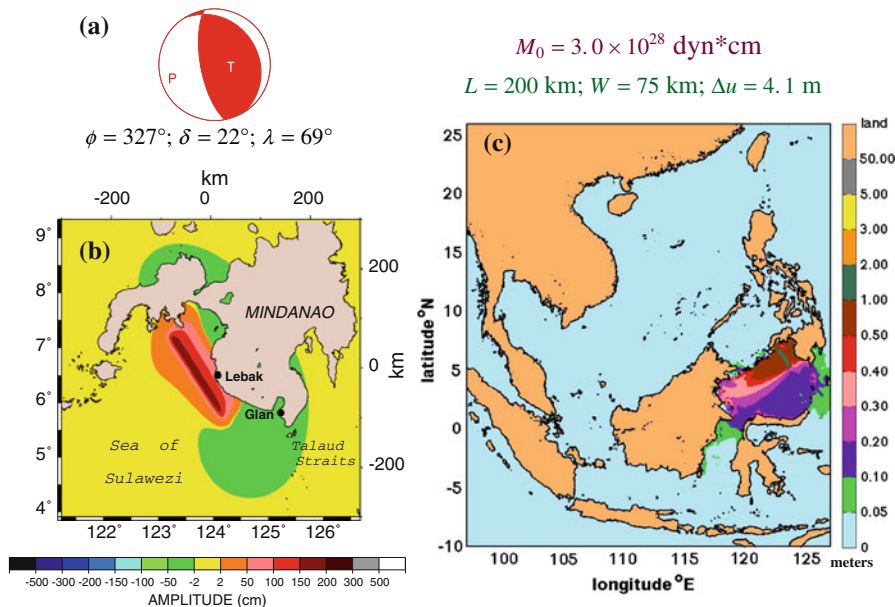


Figure 5

Same as Fig. 3 for Scenario 2 (Mindanao 1918). Note that the tsunami remains essentially contained in the Sea of Sulawesi

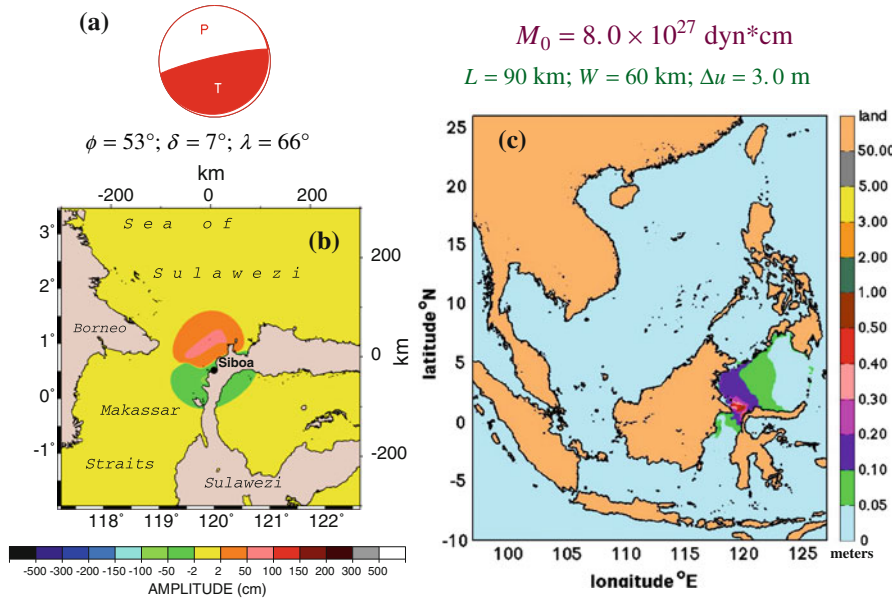


Figure 6

Same as Fig. 3 for Scenario 3 (Sulawesi 1996). Note that the tsunami remains essentially contained in the Sea of Sulawesi, with the exception of a small leak into the Makassar Straits

inside the Sea of Sulawesi. The larger moment of the 1918 earthquake is not sufficient to export substantial waves outside its basin.

3.3. Scenario 3: The 1996 Sulawesi Event

The southern shore of the Sea of Sulawesi is the locus of a small subduction system where its oceanic crust sinks under the curving Minahassa peninsula of the Island of Sulawesi. The largest CMT solution in the area is the Siboa event of 01 January 1996 ($M_0 = 7.8 \times 10^{27}$ dyn cm), expressing oblique subduction under the island. It generated a moderate tsunami, with run-up reaching 3.5 m and nine confirmed deaths (PELNOVSKY *et al.*, 1997). These results are supported by our simulation, which shows the tsunami largely confined to the northern section of the Makassar Straits (Fig. 6).

3.4. Scenario 4: A Potential Large Event in Northern Sulawesi

To the east of the 1996 epicenter, ten CMT solutions with thrusting mechanisms are available, notably between 122°E and 124°E , in the range of

$10^{25} - 3.3 \times 10^{27}$ dyn cm. While such earthquakes were apparently too small to generate reportable tsunamis, they indicate that active subduction is taking place at this margin, and raise the possibility of larger events. Indeed, four historical earthquakes are documented in the area with magnitudes assigned by GUTENBERG and RICHTER (1954) in the 7.0–8.4 range, although none of them generated reported tsunamis, and the latter (22 January 1905) cannot be associated definitely with the North Sulawesi subduction. In this framework, we consider as a plausible, although undocumented, scenario an underthrusting event rupturing the 250-km segment covered by the 10 recent (CMT) subduction earthquakes. Scaling laws suggest that it would reach $M_0 = 4.4 \times 10^{28}$ dyn cm.

Results shown in Fig. 7 show a tsunami largely contained in the Sulawesi Sea. In addition to the obvious threat to the Minahassa Peninsula, the stronger moment results in deep-water offshore amplitudes reaching 1 m off the western peninsula of Mindanao. Also, the tsunami exits the Sulawesi Sea at the Talaud Straits into the Caroline Sea, which, however, is outside the area of the present study. The weak propagation into the Molucca Sea, to the south

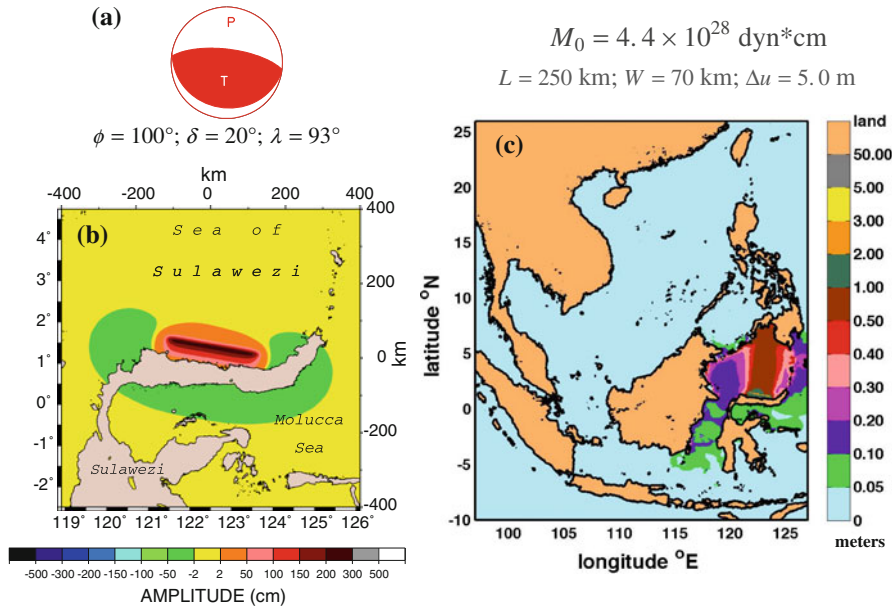


Figure 7

Same as Fig. 3 for a hypothetical large event along the north coast of Sulawesi (*Scenario 4*). Note the penetration of the straits of Makassar and Talaud

of the Minahassa peninsula expresses the extension of the field of subsidence of the earthquake south of that narrow land mass. Finally, the tsunami affects the whole coast of East Borneo, as it propagates into the Makassar Straits. However, it fails to reach the Sunda Arc across the Java Sea.

4. The Sulu Sea

4.1. Scenario 5: The 1897 Zamboanga earthquake(s)

The western peninsula of Mindanao (with its capital city, Zamboanga) and the Sulu Island chain which extends to the east of Borneo, were the site of two large earthquakes, 10 h apart, on 20 and 21 September 1897. Historical documents (CORONAS, 1899) describe a tsunami affecting the northwestern coast of Mindanao, the Sulu islands of Basilan and Jolo, and Cuyo in the north of the Sulu Sea. The tsunami killed at least 20 people, and ran up to 7 m on Basilan. Despite some confusion in timing, the tsunami can be definitely attributed to the second, stronger shock. The earthquakes were accompanied by the emergence of a small island, possibly a mud

volcano, near Labuán off the northern coast of Borneo, 700 km from the presumed epicenter; the mechanism of this ancillary phenomenon remains intriguing, especially since the earthquake was not reported as having been felt in Labuán. CORONAS (1899) also reports the emergence of another new islet near Kúdat, at the northernmost tip of Borneo, possibly associated with the *first* earthquake. In addition, SOLOV'EV and Go (1984) transcribe a report by FIGEE (1898) of the observation of a tsunami at Kúdat, and most remarkably of a “flood wave” on the east coast of Sumatra, for which, unfortunately, no further details, such as exact location and timing, are provided in the original report by FIGEE (1898).

It is all the more remarkable that these events occurred in the vicinity of the Sulu Islands, where no major earthquakes are known in the twentieth century (Fig. 2). Indeed, the largest CMT solution in the area has a moment of only 2.4×10^{24} dyn cm. GUTENBERG and RICHTER (1954) assigned magnitudes of 8.6 and 8.7 to the 1897 events. These are probably overestimated, since the absence of catastrophic reports in the southwestern Sulu Islands (Tapul group) suggests that the rupture did not extend along the full Sulu arc. In this context, we model the main

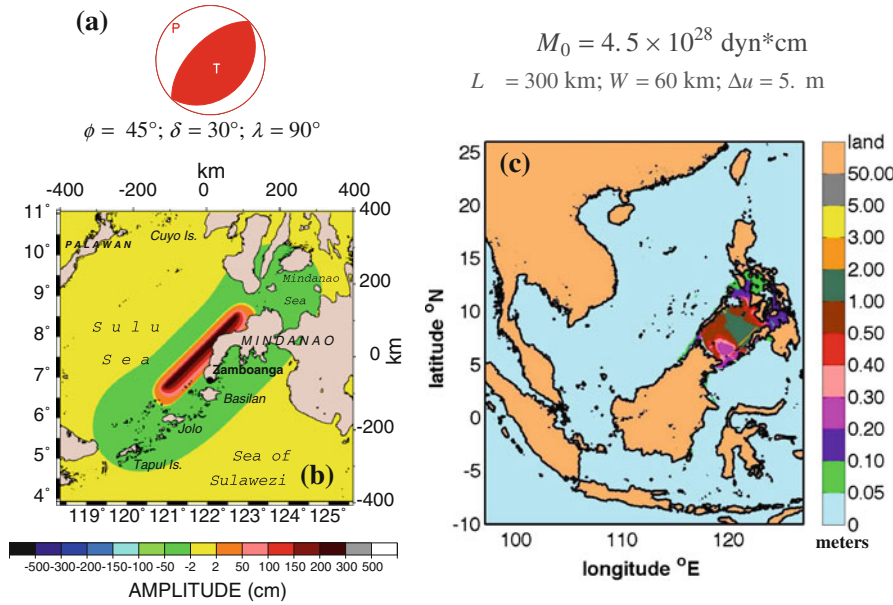


Figure 8

Same as Fig. 3 for a large event in the Sulu Sea, modeled after the 1897 earthquake (*Scenario 5*). Note that the tsunami remains confined to the Sulu Sea and the interior seas east of it. It penetrates neither the Sea of Sulawesi, nor the South China Sea

event as a 300-km rupture involving a slip of 5 m, corresponding to $M_0 = 4.5 \times 10^{28}$ dyn cm (Fig. 8). Our focal geometry is adapted from a local CMT solution (14 June 1978) by rotating the fault to conform with the orientation of the Sulu arc.

Simulation results shown in Fig. 8 indicate maximum tsunami amplitudes along the Zamboanga peninsula of Mindanao, and the eastern Sulu archipelago (Jolo, Basilan), as well as across the Sulu Sea towards Cuyo Island. The tsunami does penetrate the complex system of inner seas of the Philippine archipelago to the east of the Sulu Sea (the Mindanao Sea to the southeast and the Sibuyan Sea to the north of Panay), but does not leak into the Sea of Sulawesi south of the Sulu arc. To the north, it leaks marginally into the Balabac Straits between Palawan and Borneo, but fails to develop into the South China Sea. This model would explain the observation of a wave at Kúdat, near the Balabac Straits, but not FIGEE's (1898) reports on the east coast of Sumatra.

In this context, we considered a worst-case variant (Scenario 5a), where the fault length is extended to 500 km (and the slip accordingly scaled up to 7 m), thus rupturing the entire southern boundary of the

Sulu Sea. We emphasize that this model violates the reports (CORONAS, 1899) of a felt intensity fast decreasing to the SW in the Tapul Islands. Even so, we have verified that this model, involving the largest source that can be fit inside the Sulu Basin, cannot explain the phenomenon reported on Sumatra. In the absence of detailed information about the latter's precise location and timing, we speculate that it could represent seiching of an estuary triggered by seismic surface waves, as widely observed at comparable or even greater distances from large, or even significantly smaller, events (e.g., KVALE, 1955; CASSIDY and ROGERS, 2004; BARBEROPOULOU *et al.*, 2006).

4.2. Scenario 6: Inspired by the Iloilo, Panay Earthquake of 24 January 1948

The event of 24 January 1948 on Panay Island was assigned a magnitude $M = 8.3$ by GUTENBERG and RICHTER (1954), and is therefore often described as the strongest earthquake in the Philippines in the twentieth century. However, based on a single Pasadena record, OKAL (1992) suggested that this value was overestimated. The earthquake caused considerable damage over the island of Panay, and

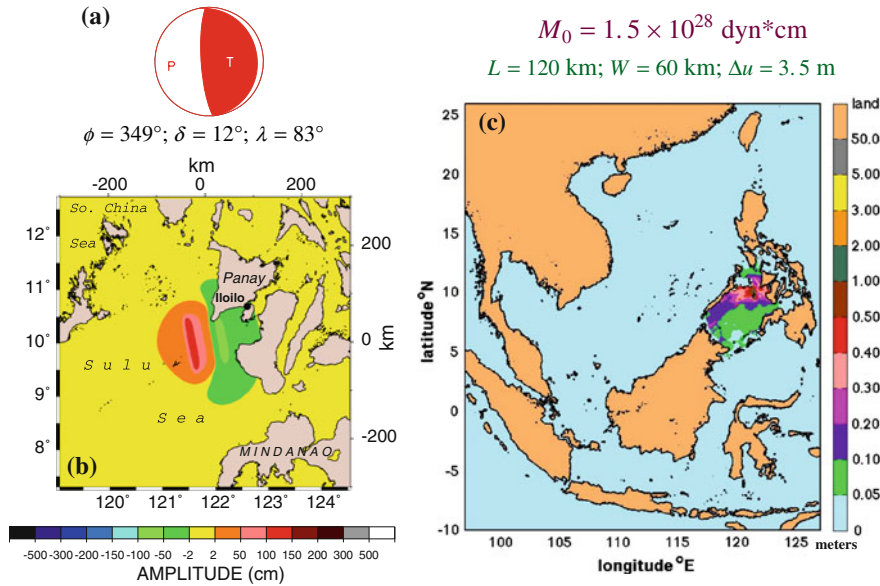


Figure 9
Same as Fig. 3 for Scenario 6. The tsunami remains contained in the Sulu Sea

triggered a small tsunami near Iloilo, with two deaths attributed to the tsunami (IRVING and TEVES, 1948).

We inverted the moment tensor of the source using long-period mantle waves recorded at Paris, Tucson, Huancayo and San Juan, through the PDFM algorithm introduced by REYMOND and OKAL (2000). This method inverts only the spectral amplitude and discards the phase information; it is especially suited to historical seismograms for which timing uncertainties could affect spectral phases (OKAL and REYMOND, 2003). The inherent indeterminacy of $\pm 180^\circ$ on both the strike and slip angles (ROMANOWICZ and SUÁREZ, 1983) can be lifted through the use of first motion polarities at critical stations. The resulting focal mechanism, shown in Fig. 9, expresses thrust faulting ($\lambda = 83^\circ$) on a plane striking $\phi = 13^\circ$, and dipping $\delta = 26^\circ$ to the east. The inverted seismic moment, $M_0 = 6 \times 10^{27}$ dyn cm, is in general agreement with OKAL's (1992) estimate, and difficult to reconcile with the published $M = 8.3$.

We consider as Scenario 6 an event of moment $M_0 = 1.5 \times 10^{28}$ dyn cm, rupturing 120 km along the trench running west of Panay Island, from Mindoro to Mindanao. This fault system has supported a much smaller earthquake of moment

1.1×10^{25} dyn cm, (05 January 1983), whose focal geometry is used for Scenario 6.

As shown in Fig. 9, our simulation yields a tsunami confined to the Sulu Sea, which fails to penetrate the South China Sea.

5. The Luzon Trench

The western shore of Luzon is generally regarded as an active subduction zone, where the Sunda plate, bearing the South China Sea, subducts under the Philippine Sea plate. This system is expressed in the bathymetry as the Luzon Trench, extending from Taiwan in the north to the Palawan Islands off Mindoro in the south (a distance of 1,200 km) and reaching a depth of 4,500 m. This interpretation is also supported by the presence of an active volcanic arc including Pinatubo and Taal Volcanoes. However, no large subduction earthquakes are known along the Luzon Trench from Taiwan to Mindoro. The largest thrust solutions in the CMT catalog are the events of 01 June 2008 near the Batan Islands at the extreme north of the system ($M_0 = 3.9 \times 10^{25}$ dyn cm) and of 29 August 1977 off northern

Luzon ($M_0 = 3.3 \times 10^{25}$ dyn cm). Such small earthquakes cannot contribute significantly to releasing the local convergence, expected to total 10 cm/year between the Sunda and Philippine plates (SELLA *et al.*, 2002).

This raises the possibility of larger subduction events along the Luzon Trench, especially given the relatively young age of the South China lithosphere off Luzon [25 Ma at 17°N (MÜLLER *et al.*, 2008)]. Indeed, catalogues of historical seismicity document a significantly larger earthquake on 14 February 1934, assigned $M = 7.9$ by GUTENBERG and RICHTER (1954), and which we examine in detail as Scenario 7. In turn, this leaves open the possibility of even larger seismic sources along the Luzon trench. No such earthquakes are documented in the instrumental seismological record of the past 100 years, nor does REPETTI's (1946) authoritative catalogue going back to the sixteenth century A.D. reveal any catastrophic tsunami on the western shore of Luzon. In this context, the occurrence of any such event remains improbable, but we do not regard it as *impossible*, and therefore consider two such mega-earthquakes as Scenarios 8 and 9.

5.1. Scenario 7: The Western Luzon Earthquake of 14 February 1934

This event took place in the vicinity of the 1977 epicenter, and generated a small tsunami on the nearby coast of Luzon, notably at San Esteban (SOLOV'EV *et al.*, 1984); unfortunately, quantified reports of its run-up are not available. The published magnitude estimate, $M = 7.9$, suggests that the event was much larger than any of the CMT solutions from the digital era. Thus, it is important to determine its exact size, focal solution, and to investigate the source of its tsunami. We will show that this event consists of an earthquake of moment $M_0 = 2.2 \times 10^{27}$ dyn cm, accompanied by an underwater landslide.

Focusing first on the seismological data, we relocated the event using the arrival times published by the ISS and the method of WYSESSON *et al.* (1991). The solution converges to 17.47°N, 119.09°W on a dataset of 138 stations, with a standard deviation of only $\sigma = 2.9$ s; the Monte Carlo ellipse ($G = 6$ s) is less than 50 km in major axis (Fig. 10a).

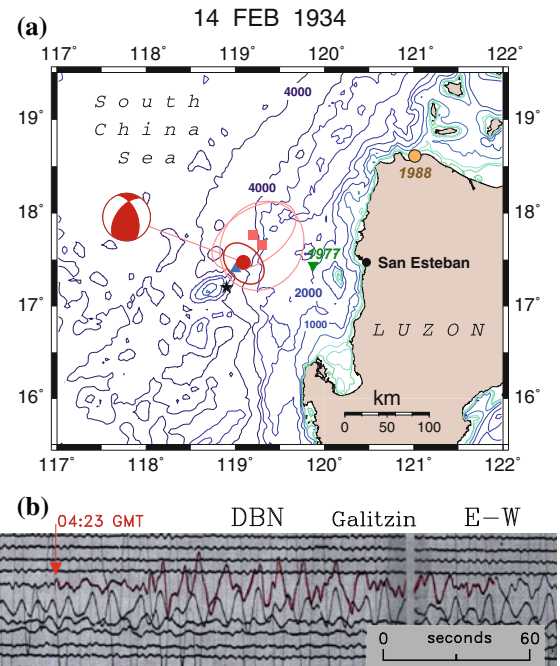


Figure 10

a Map of the epicentral area of the 1934 earthquake. The large dot is the relocated epicenter, with its Monte Carlo ellipse; the triangle is the ISS location. The faint-toned squares (with ellipses) show the relocated aftershocks of 14 February (17:14 GMT) and 25 February 1934. Note the seamount topping at 500 m b.s.l. about 40 km SW of the epicenter. The star shows the proposed location of the landslide on the flank of the seamount. The beachball at left shows the mechanism obtained by the PDFM inversion. The inverted triangle locates the largest CMT solution in the area (29 August 1977). The event of 24 June 1988 in northern Luzon is also shown.

b Close-up of the S wavetrain recorded on the East-West Galitzin instrument at De Bilt. Note the long-period oscillation lasting approximately 1.5 min after the SKS-S-ScS arrivals, which at $\Delta = 90.1^\circ$, should all be contained within 25 s

We then proceeded to invert the moment tensor of the source using long-period mantle waves recorded at De Bilt, Tucson and San Juan, through the PDFM algorithm. The resulting focal mechanism, shown in Fig. 10, can be interpreted as an oblique thrust ($\lambda = 53^\circ$) on a plane striking $\phi = 338^\circ$, and dipping $\delta = 46^\circ$ to the northeast. This mechanism also agrees well with an extensive set of first motions compiled by REPETTI (1934). The inverted seismic moment, $M_0 = 2.2 \times 10^{27}$ dyn cm, is more than 5 times the largest published CMT in the area, but fails to characterize the event as a great subduction zone earthquake. The seismic character of the event is also confirmed by its abundant aftershocks, both locally

Table 2

Observation and modeling of low-frequency phase during the Luzon event of 14 February 1934

Station		Distance (°)	Azimuth (°)	Back-Azimuth (°)	Modeled radiation patterns			Low-frequency wave
Code	Name				$ R^P $	$ R^{SV} $	$ R^{SH} $	
HKC	Hong Kong	6.68	316.9	135.2	0.99	0.07	0.10	Present on <i>P</i> phase
PLV	Phu-Lien, Vietnam	12.23	287.8	103.6	0.88	0.31	0.37	Present on <i>P</i> phase
ZKW	Zi-ka-wei, China	13.84	8.4	189.4	0.50	0.23	0.84	Present on <i>S</i> phase
KOC	Kochi, Japan	22.15	32.7	219.2	0.01	0.10	1.00	Present on <i>S</i> phase
PEK	Chiufeng (Beijing), China	22.67	354.2	172.8	0.47	0.55	0.69	Absent
DBN ^a	De Bilt, The Netherlands	90.13	325.7	60.6	0.25	0.93	0.27	Present on <i>S</i> phase (EW)

^a This study

detected as reported by REPETTI (1934) (36 shocks over 3 days), and telesismically recorded (2 shocks over 12 days).

However, evidence clearly points to the triggering of a landslide by this earthquake. Most significantly, the event resulted in the rupture of telegraphic cables in the South China Sea; upon their repair, significant changes were documented in the seafloor topography (REPETTI, 1934), which is the clear mark of an underwater landslide, as documented in the case of similar ruptures off the Grand Banks of Newfoundland (18 November 1929), the northern coast of Algeria (9 September 1954, 10 October 1980 and presumably 21 May 2003), and the southern coast of Fiji (14 September 1953) (HEEZEN and EWING, 1952, 1955; HOUTZ, 1962; EL-ROBRINI *et al.*, 1985; BOUHADAD *et al.*, 2004).

In addition, REPETTI (1934) describes, unfortunately without figures, a long-period (13–22 s) wave, of an “unknown exact nature”, lasting about 1 min and appearing shortly after the *P* wave on seismograms at Hong Kong and Phu-Lien, and at the time of the *S* arrival (or shortly thereafter) at Zi-ka Wei and Kochi. He further mentions that seismograms at Chiufeng (Beijing) are “normal”, i.e., do not feature this long-period wave, but does not comment on its observation (or absence) at greater distances. Among the seismograms available to us, we were able to document a particularly long-lasting *S* wavetrain on the East–West component at De Bilt (Fig. 10b) which would appear to share the characteristics of REPETTI’s (1934) observations in terms of period and duration.

The records of these long-period wave trains, summarized in Table 2, can be interpreted as the

P and *S* waves of an ancillary source, namely a landslide essentially coeval with the earthquake. In Fig. 10a, we note that the earthquake relocates to the immediate vicinity (40 km) of a major seamount with relatively steep slopes, which the seismic dislocation could have destabilized. We propose that a landslide was initiated on the eastern side of the seamount, and generated a turbidity current which broke the nearby Manila–Shanghai cable, as reported by REPETTI (1934). In Table 2, we further use the formalism of Equation (1) of KANAMORI *et al.* (1984) to compute the relevant radiation pattern coefficients of the *P* and *S* waves of the landslide source, modeled as a subhorizontal force ($\delta = 4^\circ$) in the azimuth $\phi_f = 130^\circ$. Apart from Chiufeng, the agreement is excellent: those stations (HKC and PLV; at short distance and in the azimuth of the force) where the “long” wave appears with the *P* phase are precisely those where the landslide *P* wave is expected to be strongest and the *S* wave minimal, and conversely at ZKW, KOC, DBN (at large distance or at right angle to the force). At DBN, we verify that the *S* arrival is prominent on the EW component, approaching SV polarization.

We conduct two separate simulations of the tsunami generated by the 1934 earthquake. In Scenario 7a, we use the dislocation source; in Scenario 7b, we consider a landslide source, using a dipolar initial deformation of the sea surface consisting of a 19-m deep trough and a 16-m high hump, separated by a 22-km lever. The size of the poles is inspired from those used to model the 1998 Papua New Guinea tsunami (SYNOLAKIS *et al.*, 2002), but the lever is lengthened since the Papua New Guinea slide took place in a confined amphitheater. In the absence of

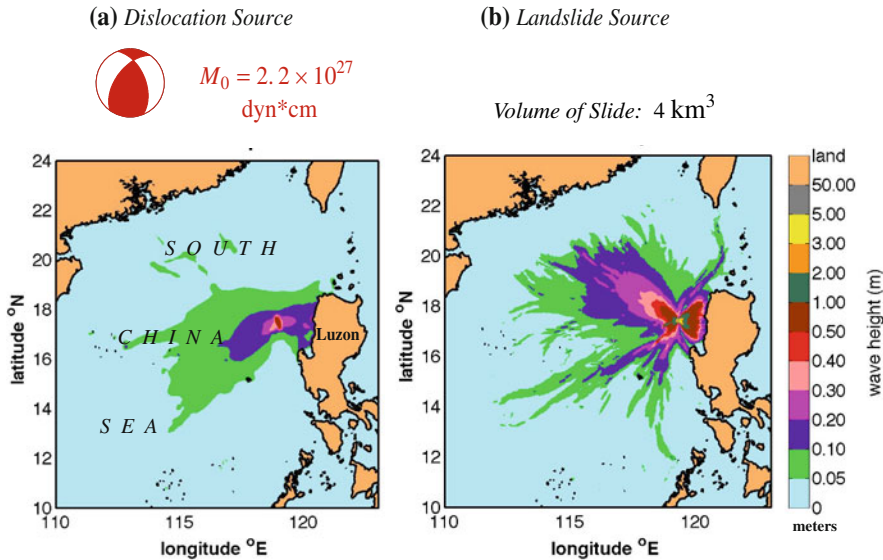


Figure 11

Simulations for Scenarios 7 (West Luzon earthquake of 14 February 1934), using **a** the dislocation source inverted in this study (see Fig. 10), and **b** a landslide source inspired by the 1998 Papua New Guinea event. The scale is common to both frames

details on the geometry of the landslide, we regard this model as a compromise between the need for a substantial slide detected teleseismically, and the relatively minor tsunami described qualitatively by REPETTI (1934). Our simulations shown in Fig. 11 show that the tsunami from the dislocation source reaches the Luzon shore with deep-water amplitudes of ~ 0.1 m, while the landslide simulation is not much larger; neither of them threatens distant shores in the South China Sea.

The possibility of even moderate earthquakes along the northwestern coast of the Philippines generating tsunamis through the triggering of landslides is further suggested by the small earthquake of 24 June 1988 in Bangui, northern Luzon ($m_b = 5.4$; $M_0 = 3.7 \times 10^{24}$ dyn cm), which generated the largest tsunami wave recorded in Hong Kong (1 m). We note the steepness of the bathymetry in its epicentral area, which could suggest the triggering of a significantly larger landslide than in 1934.

5.2. Scenarios 8 and 9: Catastrophic Earthquakes at the Luzon Trench

We consider in this section the possibility that the Luzon Trench could support mega-earthquakes with a

moment reaching 10^{29} dyn cm. We wish to re-emphasize that no such earthquakes are documented in the seismological record (including historical reports) available to us. However, we cannot entirely forgo the possibility that they could actually take place, with an extremely long recurrence time. A similar paradigm existed in Cascadia prior to the identification of the 1700 earthquake (SATAKE *et al.*, 1996), or to a large extent along the Andaman-Nicobar segment of the Sumatra Trench prior to 2004. Further research on paleo-tsunamis using sedimentological techniques could confirm or infirm this hypothesis in the case of the Luzon Trench.

It is in this context that we consider in Scenario 8 an event rupturing the full 400 km of the Luzon Straits from the southern tip of Taiwan to the northern tip of Luzon, and in Scenario 9 an event of similar size rupturing along the western shore of Luzon. Source parameters for these events are derived from scaling laws with geometries inspired by the local tectonics. All relevant parameters are listed in Table 1, with results shown in Figs. 12 and 13. Our source for Scenario 9 is smaller than that considered by MEGAWATI *et al.* (2009), since we restrict ourselves to a reasonably linear fault zone.

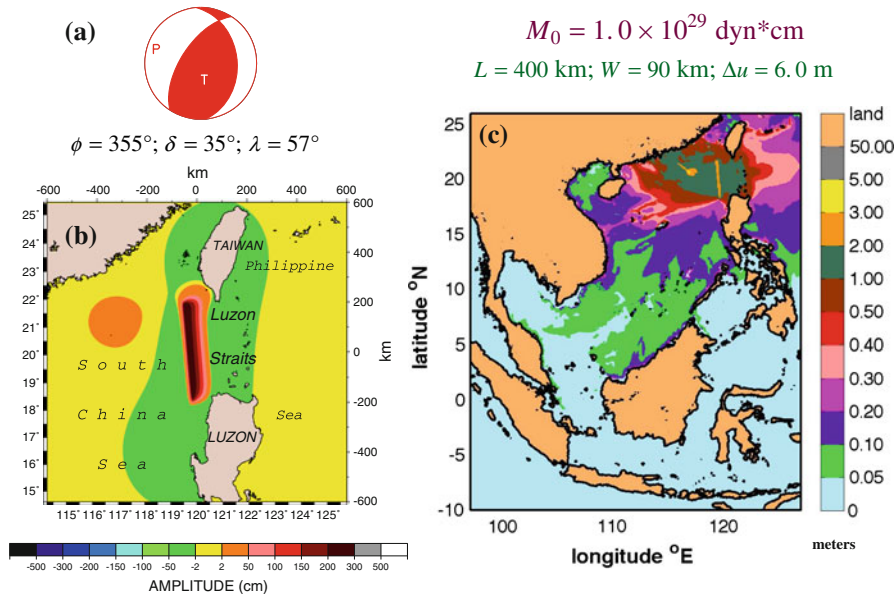


Figure 12

Same as Fig. 3 for hypothetical Scenario 8, a catastrophic earthquake rupturing the full length of the Luzon Straits. Note that the tsunami has very high amplitudes over all of the South China Sea (with the exception of the Gulf of Thailand) and leaks into the Philippine Sea, but does not penetrate the Sulu Sea or the interior seas of the Philippine archipelago

As expected, the size of the events results in catastrophic levels of hazards. Under Scenario 8, all shores of the South China Sea are threatened. Metric deep-water amplitudes are predicted for the southern coast of China around Hong Kong. Expectedly, the tsunami leaks through the Luzon Straits into the Philippine Sea, affecting the eastern coast of Taiwan and the Ryukyu archipelago, and even the eastern coast of Luzon. It keeps at most centrimetric amplitudes in the Gulf of Thailand, but could become noticeable along the northern shore of the Malay Peninsula. Under Scenario 9, results are generally similar, but the western coast of Luzon obviously bears the onslaught of the tsunami, while source directivity and focusing by bathymetric features combine to displace the brunt of the attack from southern China to Vietnam and, albeit more moderately, to the northern coast of Borneo. In addition, the Malay peninsula is clearly threatened at the latitude of the Narathiwat and Pattani provinces of southern Thailand (Fig. 13).

However, a remarkable result of our simulations is that, even for those catastrophic, and perhaps unrealistic sources, the tsunami does not penetrate the Sulu Sea, except for very minor leaks at the Mindoro

and Balabac Straits. Similarly, under Scenario 9, the Luzon Straits remain, by and large, an effective barrier.

6. Taiwan Straits Events

Historical records document a number of catastrophic events in the Taiwan Straits which generated locally severe tsunamis. While no record exists (to our knowledge) of the propagation of these tsunamis into the South China Sea, it is legitimate to examine and simulate these sources in order to assess their potential threat to our study area. We base our discussion on the review by MA and LEE (1997).

6.1. Scenario 10: The Hsinchu Event of 29 December 1604

This major intraplate earthquake took place in Fujian Province and caused considerable destruction over a 700-km section of coastline, from Shanngyu in the north to Zhangpu in the south. ZHOU and ADAMS (1988) indicate that a tsunami affected the mainland, but to our knowledge, no such reports exist for

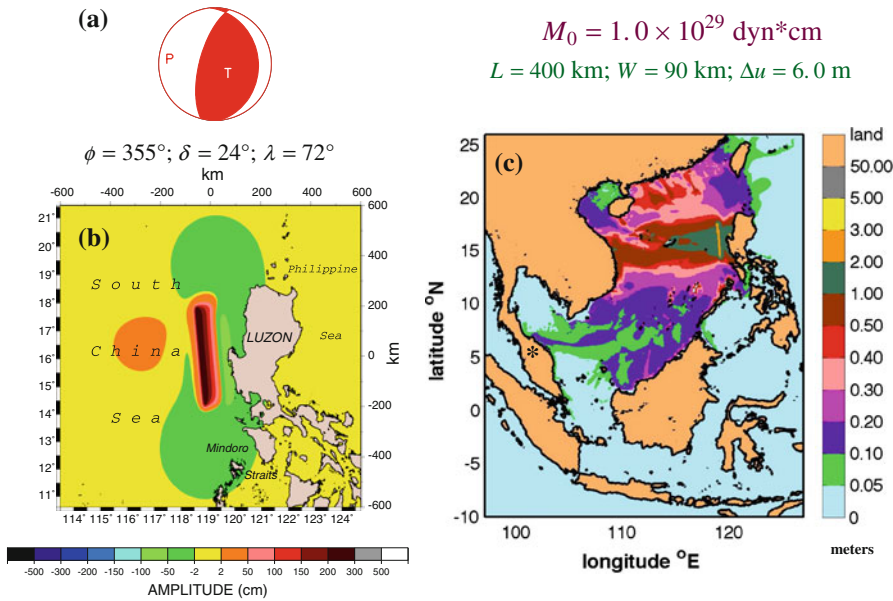


Figure 13

Same as Fig. 3 for hypothetical Scenario 9, a catastrophic earthquake at the Luzon Trench, off the western shore of the island. The results are generally similar to those of Scenario 8, with the exception of stronger effects on the coast of Borneo, higher amplitudes in Narathiwat and Pattani provinces in Thailand (asterisk), but no penetration of the Philippine Sea

Taiwan. Isoseismals compiled by YE *et al.* (1993) suggest a fault line of ~ 150 km, which B.S Huang (pers. com, 2003) has interpreted in terms of a moment of $\sim 3 \times 10^{27}$ dyn cm. As a worst-case scenario, we use in our simulation $M_0 = 10^{28}$ dyn cm, with a pure 45° -thrust geometry along the general strike of the straits ($\phi = 50^\circ$). Our results (Fig. 14) do predict significant wave heights off the mainland coast and to a lesser extent Taiwan, but the tsunami fails to penetrate either the East or South China Seas.

6.2. Scenario 11: The Fo-kien earthquake of 22 May (or October?) 1782

Reports from travelers describe a catastrophic tsunami causing up to 40,000 deaths in Taiwan and destroying the forts of Zelandia (presently Tainan) and Pingkchingi (GAZETTE DE FRANCE, 1783), although claims of the island being “nearly entirely covered” (by water) are clearly fanciful. There is some discrepancy on the date of the event which may also have been accompanied—or triggered—by a volcanic eruption. In the absence of more definitive information on the earthquake (incidentally, absent from MA and LEE’s (1997) compilation), we simply

move the source of Scenario 10 across the straits, off the coast of Taiwan. Since it is probable that the 1782 earthquake took place in the general area of the Taiwan Straits, Scenarios 10 and 11 can represent geographic endmembers for potential sources in the straits. Our results, shown in Fig. 15, are essentially unchanged, i.e., the tsunami does not propagate significantly outside the straits.

6.3. Scenario 12: The Tainan earthquake of 08 January 1661

This catastrophic event was described in detail by SCHOUTEN (1725), suggesting a destructive tsunami in the Fort Zelandia (Tainan) area, with run-up probably greater than the 1–2 m suggested by HSU (1996) and modeled by MA and LEE (1997), perhaps as a consequence of triggered submarine landslides.

Following MA and LEE (1997), we place the source of the event used in our simulation in the seismically active belt around 22°N , 119°E , but give it the normal faulting mechanism of the largest CMT in the area (16 September 1994). Under a worst-case scenario, we boost the moment to 1.5×10^{28} dyn cm, with a fault length (127 km)

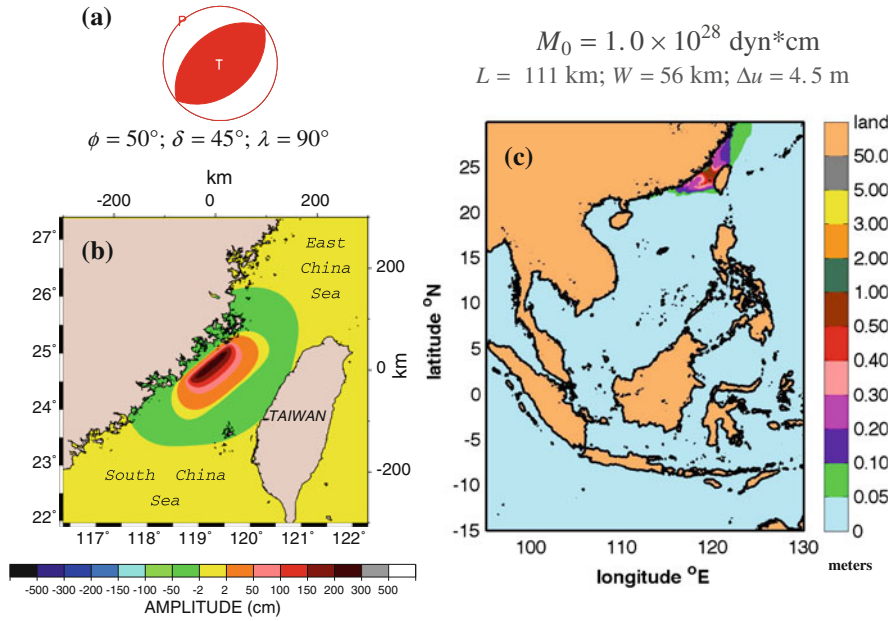


Figure 14

Same as Fig. 3 for Scenario 10, a major earthquake along the mainland coast of the Taiwan Straits, inspired by the 1604 Hsinchu earthquake.
Note that the tsunami remains contained in the straits

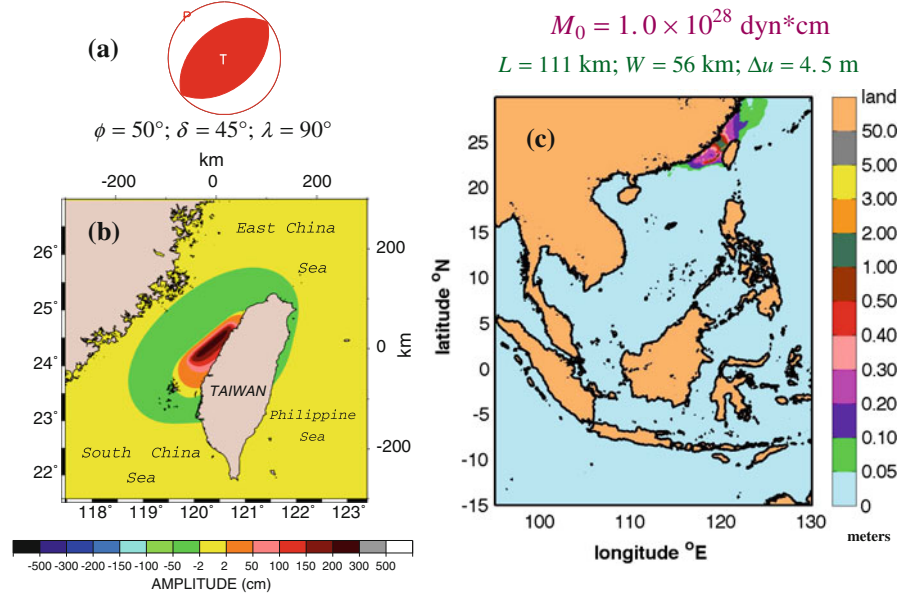


Figure 15

Same as Fig. 14 for Scenario 11, where the earthquake is displaced towards the coast of Taiwan, as inspired by reports of the 1782 event. The far-field effects of the tsunami are unchanged

representative of the local extent of seismicity. Our results show very strong amplitudes along the southwestern coast of Taiwan, in the area of Tainan, and in the mainland coastal region, as far south as

Hong Kong and Hainan. Significantly, the tsunami also extends into the East China Sea, and affects the northern coast of Luzon, the Palawan Islands and possibly the central coast of Vietnam (Fig. 16).

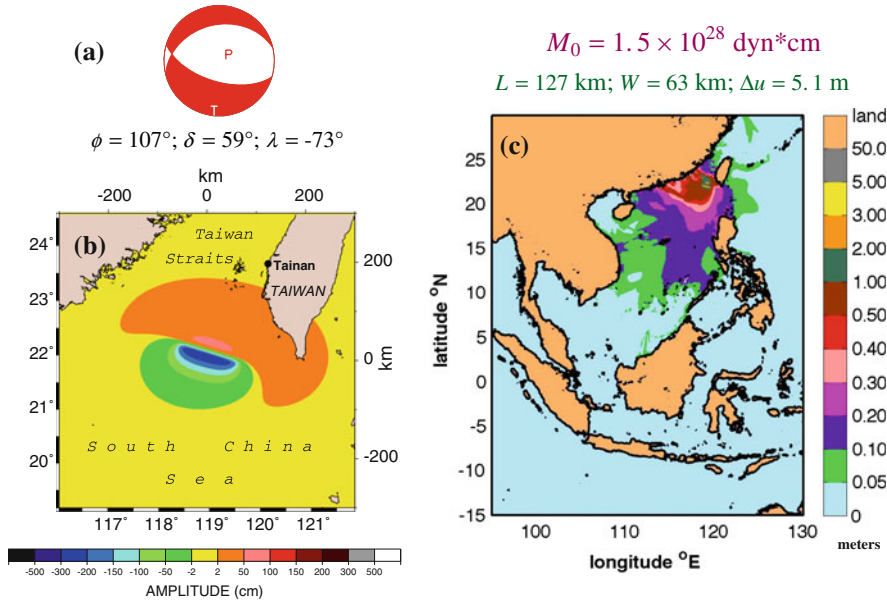


Figure 16

Same as Fig. 14 for Scenario 12, inspired by the 1661 event. As the earthquake is moved to a deep-water environment, the tsunami is able to expand into the South China Sea, and threatens the coasts of Hainan, Vietnam and Palawan

This difference in behavior, relative to Scenarios 10 and 11, is a classical illustration of GREEN'S (1837) law. In the latter two, the tsunami is generated in extremely shallow water, the Taiwan straits being in general less than 100 m deep. When attempting to penetrate the East China Sea, where depths reach several thousand meters, the tsunami falters. A similar result was obtained in Paper I under its Scenarios 3 and 4, whose sources located in the shallow Bay of Bengal remained benign in the far-field deep basins of the Indian Ocean. By contrast, in Scenario 12, the source is already in deep water, and the tsunami propagates efficiently across the deep South China Sea basin.

7. Danger from the Indian Ocean?

In this section, we examine the possibility of a significant tsunami penetrating into the South China Sea and its adjoining basins from outside, and focus on possible sources located in the Indian Ocean.

During the 2004 Sumatra-Andaman earthquake, no significant tsunami was reported inside our study area, expressing the convoluted and inefficient path

such waves would have had to take through the straits of Malacca. Similarly, during the 1994 and 2006 Java “tsunami earthquakes”, whose run-ups reached 14 m and 21 m, respectively, on the southern coast of Java (TSUJI *et al.*, 1995; FRITZ *et al.*, 2007), no tsunami was detected in the Java Sea.

To complement these observations, we examine here as Scenario 13 the case of a hypothetical mega-thrust event south of Java, namely Scenario 8 of Paper I, consisting of a 500-km rupture south of Java, with a moment of 3.6×10^{29} dyn cm. We emphasize, once again, that such events are undocumented in the Java Trench, and indeed, most improbable. However, as argued in Paper I, they may not be totally *impossible*, and as such we carry out this simulation, in the same spirit as for Scenarios 8 and 9 in western Luzon.

Results shown in Fig. 17 show that the tsunami fails to propagate significantly into the Java Sea. It features only a small leak through the Straits of Bali and Lombok, and essentially none at the Sunda Straits. Given the documented absence of penetration in 2004, and the shelter provided by the island of Sumatra for tsunamis generated along its central and southern segments [e.g., in the geometry of the 1833

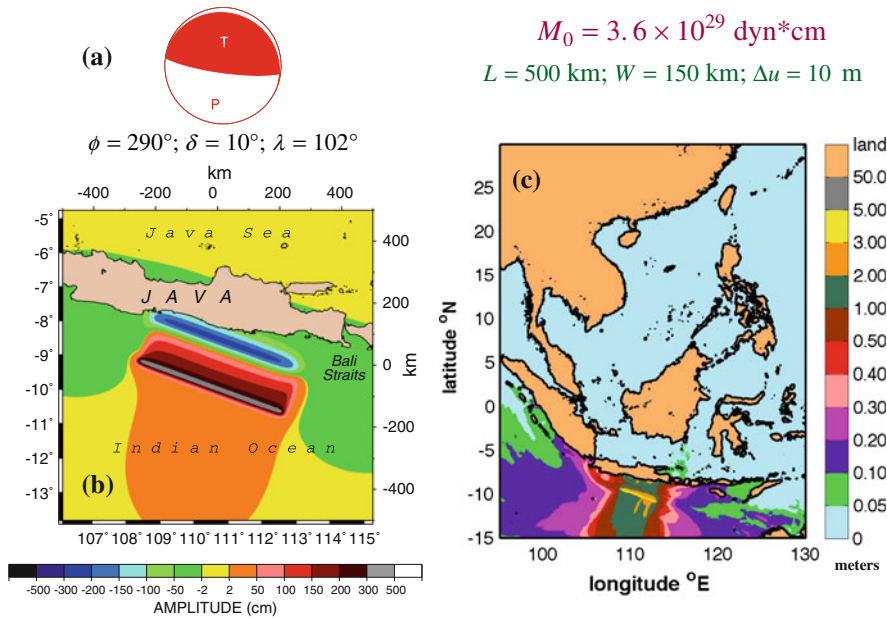


Figure 17

Same as Fig. 3 for Scenario 13 (hypothetical mega-thrust event south of Java). Note that the tsunami hardly penetrates into the Java Sea at the Bali Straits

Mentawai earthquake (ZACHARIASEN *et al.*, 1999)], we conclude that Indian Ocean tsunamis cannot significantly affect the South China Sea and its adjoining basins.

Finally, the largest transpacific tsunamis (Peru, 1868; Chile, 1960) were observed at decimetric amplitudes in the Philippines, without, however, reaching damaging levels. No mega-earthquakes are known at a regional distance in the Pacific Basin (e.g., Ryukyu; East Luzon); while their possibility cannot be totally discounted, they remain improbable and transcend the scope of this paper.

8. The Case of the Brunei Slide

Finally, we investigate in this section the scenario of a catastrophic landslide occurring inside the South China Sea Basin. We are motivated by the work of GEE *et al.* (2007), who used 3-dimensional seismic imaging to document the presence of such a structure off the coast of Brunei, at the delta of the Baram River (Fig. 2). Its estimated volume, $1,200 \text{ km}^3$, makes it one of the largest underwater slides in the world, comparable to the Saharan and Hinlopen

slides (EMBLEY, 1976; VANNESTE *et al.*, 2006), and as much as one-third the volume of the record Storrega slide (BUGGE *et al.*, 1988). However, the Brunei Slide is unique in being “thicker”, i.e., differing in aspect ratio from the other mega-slides, and in occurring in an environment with abundant sediment flux from the Baram River. The age of the Brunei slide is debated, but it could be as recent as Holocene, while deeper structures in the seismic stratigraphy suggest repeated episodes of sliding (GEE *et al.*, 2007). In this context, the Brunei slide might be reactivated in the future, and should be included as a source of tsunami hazard in the South China Sea.

We consider in Scenario 14 a model of the Brunei Slide using a dipolar source with a 90-m trough and a 60-m hump, separated by an 80-km lever. These numbers are obtained by scaling the Papua New Guinea dipole (SYNOLAKIS *et al.*, 2002) to the expected thickness and movement of the Brunei slide, while constraining the length of the lever to its mapped extent. Results, shown in Fig. 18, show deep-water amplitudes reaching 5 m on the nearby coast of Borneo (which would lead to complete devastation) and approaching 1 m along the coast of Vietnam. Although, as expected from its shorter

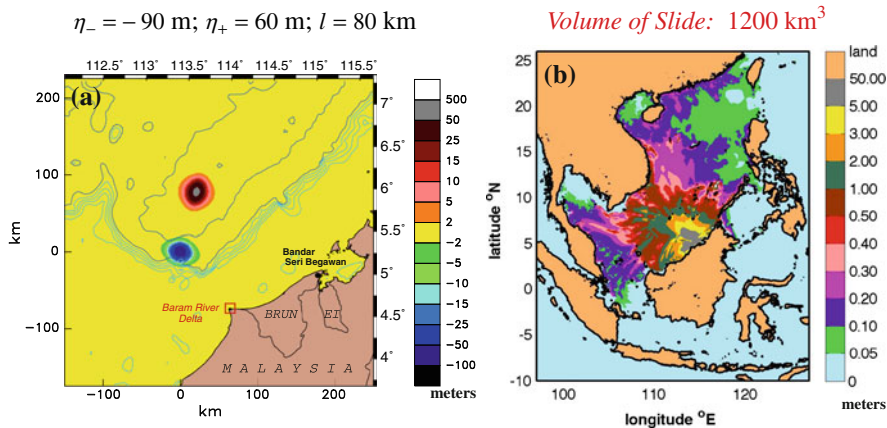


Figure 18

Simulation of the Brunei monster slide. **a** Field of initial displacements. The model consists of a dipole oriented N15°E along the slope of the South China Sea Basin. **b** Maximum simulated wave height reached in the study area. Note catastrophic deep-water amplitudes in the central part of the basin

wavelengths, the tsunami disperses quickly in the far field, amplitudes in deep water off Luzon, the southern coast of China and southern Taiwan remain decimetric, and could lead to damage upon run-up. Significant inundation is expected along the Palawan Islands, but the tsunami leaks only moderately into the Sulu Sea along the Malaysian coast of Borneo. It remains decimetric as it approaches the northern coast of the Malay peninsula, with the potential for damage along most of its shores. However, the tsunami does not reach the Java Sea.

The mechanism of triggering of the Brunei slide remains unknown; GEE *et al.*, (2007) have suggested as possible agents intraplate earthquake activity, anticline collapse or the destabilization of gas hydrates, as suggested for example by BOURIAK *et al.*, (2000) at the Storrega site in the context of the Fennoscandian deglaciation. We note the occurrence on 21 July 1930 of an earthquake assigned $M = 6$ by GUTENBERG and RICHTER (1954), in the center of the South China Sea basin, which we relocated to 7.92° and 113.48°E (Fig. 2), in a deep portion of the South China Basin, and approximately 120 km north of the toe of the Brunei Slide. While the earthquake is too small to be successfully studied on the basis of historical seismograms, the magnitude proposed by GUTENBERG and RICHTER (1954) could be sufficient, especially given its intraplate character, to create accelerations inducing landslides along ridge structures located 50 km to the southeast. A larger

earthquake at the same location could conceivably trigger the motion of a precarious structure in the general area of the Brunei slide. In addition, we note that other river systems provide sedimentary fluxes into the South China Basin along the north coast of Borneo. Thus, the risk of a Brunei-type slide may be present along all of the northern half of the coast of Borneo, where the South China Sea features a deep oceanic basin.

9. Discussion and Conclusion

The principal results from this study can be summarized as follows:

- With the exception of the complex system of interior seas of the western shores of the Philippines, our simulated scenarios generally result in containment of the tsunamis to their original individual basin. The Palawan–Calamian system on the one hand, and the Sulu archipelago on the other, make up effective barriers preventing the propagation of tsunamis from one basin to the next. The Luzon straits separating Taiwan from the Philippines, and the Talaud straits joining the Sulawesi Basin with the Philippine Sea, are expectedly less effective, and allow some leakage of energy. The Makassar Straits also damp considerably the amplitude of waves crossing them.

These results, largely documented from historical tsunamis, remain robust when worst-case scenarios featuring improbable, but perhaps not impossible, seismic moments, are considered in the simulations. By the same token, Indian Ocean tsunamis cannot penetrate into the South China Sea, through the narrow Bali and Sunda Straits.

- In addition, the extensive very shallow bathymetry comprising the western part of the South China Basin and the Java Sea acts to dampen regional tsunamis propagating from the deeper basins in the eastern South China Sea and across the Straits of Makassar, with the result that the relevant shorelines in the Gulf of Thailand, and the eastern shores of Sumatra, the western and southern coasts of Borneo, and the north coast of Java are not inundated under most of our tectonic scenarios. Only for the improbable mega-thrust event off western Luzon (Scenario 9) and for the catastrophic Brunei slide (Scenario 14) are the northern shores of the Malay Peninsula threatened. A comparison of Figs. 13 and 18 reveals that in both cases the largest amplitudes are found offshore from the southern-most provinces of Narathiwat and Pattani in Thailand. This is probably due to the focusing effect of a domain of extremely shallow bathymetry directly offshore of these locations, where we have verified that the 50-m isobath extends more than 150 km into the Gulf of Thailand.

On the other hand, the intriguing report by FIGEE (1898) of a flood wave in Sumatra during the 1897 Sulu event could not be explained under any acceptable scenario for its source, and we speculate that it may have resulted from a seiche in an estuary, triggered by seismic surface waves of large amplitude.

- The modern seismological record clearly underestimates the tsunami potential in the region. No significant recent earthquake is known along the Sulu arc, in the epicentral area of the 1897 shock. Modern analyses of historical seismograms show that the events of 1918 in the Moro Gulf and 1934 off Luzon are significantly larger than their modern counterparts. Historical chronicles in Taiwan and mainland China also provide convincing evidence of earthquakes much larger than instrumentally recorded, and accompanied by damaging tsunamis.

Such events will be repeated, even if we presently do not understand their recurrence times.

- In this respect, and by contrast with the smaller adjoining seas, the South China Sea Basin is large enough that it can accommodate the fault line of a mega earthquake, such as envisioned in Scenarios 8 and 9, and propagate its tsunamis over at least 1,500 km, a distance beyond the reach of felt seismic waves, even from the largest earthquakes, and as such often taken as separating near-field and far-field tsunamis for the purpose of warning and mitigation. In short, some shores of the South China Sea, most notably the southern Chinese mainland from the Taiwan straits to Hainan and the Gulf of Tonkin, Vietnam, and northern Borneo may feature far-field tsunami risk under Scenarios 8, 9, and 12, which are certainly most improbable, but should not be considered impossible.
- Significant tsunami risk from underwater landslides exists in the South China Sea Basin, as documented both in modern and geological history. The recent example of the 1998 Papua New Guinea disaster (SYNOLAKIS *et al.*, 2002) should re-emphasize that even moderate earthquakes (typically around magnitude 6), can trigger submarine slides creating locally catastrophic tsunamis. Such earthquakes are documented even along apparently passive margins, e.g., the 1930 shock shown in Fig. 2, in an area where the monstrous Brunei Slide points out to a geological environment generally favoring the accumulation of precarious sediment masses.
- Notwithstanding the worst-case scenarios that we have studied systematically, the most probable form of tsunami hazard along the shorelines of the South China Sea and its adjoining basins remains a large earthquake ($\approx 10^{28}$ dyn cm), rupturing one of the many active shorter fault systems in this extremely complex region. As exemplified by Scenario 1, such sources have the potential for a tsunami of disastrous dimension, especially in view of the ever-growing population along the relevant shorelines. Because of the general effectiveness of the barriers separating the various basins, such a tsunami will be mostly of near-field character; the populations at risk having little if any time to get out of harm's way. In this context, self-evacuation

will be the only practical form of mitigation, and it remains an absolute priority to emphasize awareness and education, which have proven repeatedly to be the key to reducing human losses in the near field (CAMILADE *et al.*, 2000; FRITZ and KALLIGERIS, 2008; OKAL *et al.*, 2010).

Acknowledgments

This research was partially supported by the National Science Foundation under grant CMMI 09-28905 to CES. We are grateful to James Dewey, Steve Kirby, Bernard Dost and Phil Cummins for access to historical seismogram collections at the USGS (Golden), the Royal Netherlands Meteorological Institute, and Geoscience Australia. The paper was improved through the comments of Hermann Fritz, another reviewer and Editor Utku Kanoğlu. Maps were drawn using the GMT software (WESSEL and SMITH, 1991).

REFERENCES

- ANDO, M., *Source mechanism and tectonic significance of historical earthquakes along the Nankai Trough, Japan*, Tectonophysics, 27, 119–140, 1975.
- BARBEROPOLOU, A., A. QAMAR, T.L. PRATT, and W.P. STEELE, *Long-period effects of the Denali earthquake on water bodies in the Puget Lowland: Observations and modeling*, Bull. Seismol. Soc. Amer., 96, 519–535, 2006.
- BOUHADAD, Y., A. NOUR, A. SLIMANI, N. LAOUAMI, and D. BELHAI, *The Boumerdes (Algeria) earthquake of May 21, 2003 ($M_w = 6.8$): Ground deformation and intensity*, J. Seismol., 8, 497–506, 2004.
- BOURIAK, S., M. VANNESTE, and A. SAOUTKINE, *Inferred gas hydrates and clay diapirs near the Storrega Slide on the Southern edge of the Voring Plateau, offshore Norway*, Mar. Geol., 163, 125–148, 2000.
- BUGGE, T., R.H. BELDERSON, and N.H. KENYON, *The Storrega slide*, Phil. Trans. Roy. Soc. (London), 325, 357–388, 1988.
- CAMILADE, J.-P., D. CHARLIE, U. KANOĞLU, S. KOSHIMURA, H. MATSUMOTO, A. MOORE, C. RUSCHER, C.E. SYNOLAKIS, and T. TAKAHASHI, *Vanuatu earthquake and tsunami cause much damage, few casualties*, Eos, Trans. Amer. Geophys. Un., 81, 641 and 646–647, 2000.
- CASSIDY, J. F., and G. C. ROGERS, *The $M_w = 7.9$ Alaska earthquake of 3 November 2002: Felt reports and unusual effects across western Canada*, Bull. Seismol. Soc. Amer., 94, S53–S58, 2004.
- CISTERNAS, M., B.F. ATWATER, F. TORREJÓN, Y. SAWAI, G. MACHUCA, M. LAGOS, A. EIPERT, C. YOULTON, I. SALGADO, T. KAMATAKI, M. SHISHIKURA, C.P. RAJENDRAN, J.K. MALIK, Y. RIZAL, and M. HUSNI, *Predecessors of the giant 1960 Chile earthquake*, Nature, 437, 404–407, 2005.
- CORONAS, J., *La actividad seísmica en el archipiélago Filipino durante el año 1897*, Observatorio de Manila, 129 pp., Manila, 1899.
- EKSTRÖM, G., and M. NETTLES, *Calibration of the HGLP seismograph network and centroid-moment tensor analysis of significant earthquakes of 1976*, Phys. Earth Planet. Inter., 101, 219–243, 1997.
- EL-ROBRINI, M., M. GENESSEAU, and A. MAUFFRET, *Consequences of the El-Asnam earthquakes: Turbidity currents and slumps on the Algerian margin (Western Mediterranean)*, Geo-Marine Letts., 5, 171–176, 1985.
- EMBLEY, *New evidence for the occurrence of debris flow deposits in the deep sea*, Geology, 4, 371–374, 1976.
- FIGEE, S., *Vulkanische verschijnselen en aardbevingen in den O.I. Archipel waargenomen gedurende het jaar 1897*, Natuurkundig Tijdschrift voor Nederlandsch-Indië, 58, 137–162, 1898.
- FRITZ, H.M., and N. KALLIGERIS, *Ancestral heritage saves tribes during 1 April 2007 Solomon Islands tsunami*, Geophys. Res. Letts., 35, (I), L01607, 5 pp., 2008.
- FRITZ, H.M., W. KONGKO, A. MOORE, B. MCADOO, J. GOFF, C. HARBITZ, B. USLU, N. KALLIGERIS, D. SUTEJA, K. KALSUM, V.V. TITOV, A. GUSMAN, H. LATIEF, E. SANTOSO, S. SUJOKO, D. DJULKARNAEN, H. SUNENDAR, and C.E. SYNOLAKIS, *Extreme run-up from the 17 July 2006 Java, Tsunami*, Geophys. Res. Letts., 34, (12), L12602, 4 pp., 2007.
- GAZETTE DE FRANCE, *Organe officiel du Gouvernement Royal*, Paris, 12 août 1783.
- GEE, M.J.R., H.S. UY, J. WARREN, C.K. MORLEY, and J.J. LAMBIASE, *The Brunei Slide: A giant marine slide on the Northwest Borneo Margin revealed by 3-D seismic data*, Mar. Geol., 246, 9–23, 2007.
- GELLER, R.J., and H. KANAMORI, *Magnitudes of great shallow earthquakes from 1904 to 1952*, Bull. Seismol. Soc. Amer., 67, 587–598, 1977.
- GELLER, R.J., *Scaling relations for earthquake source parameters and magnitudes*, Bull. Seismol. Soc. Amer., 66, 1501–1523, 1976.
- GODUNOV, S.K., *Finite difference methods for numerical computations of discontinuous solutions of the equations of fluid dynamics*, Matemat. Sbornik, 47, 271–295, 1959.
- GREEN, G., *On the motion of waves in a variable canal of small depth*, Cambridge Phil. Trans., 6, 457–462, 1837.
- GUTENBERG, B., and C.F. RICHTER, *Seismicity of the Earth and associated phenomena* (Princeton University Press, 1954), 310 pp.
- HAMILTON, W., *Tectonics of the Indonesian region*, U.S. Geol. Surv. Prof. Paper, 1078, 345 pp., 1979.
- HEESEN, B.C., and W.M. EWING, *Turbidity currents and submarine slumps, and the 1929 Grand Banks earthquake*, Amer. J. Sci., 250, 849–878, 1952.
- HEESEN, B.C., and W.M. EWING, *Orléansville earthquake and turbidity currents*, Bull. Amer. Soc. Petrol. Geol., 39, 2505–2514, 1955.
- HOUTZ, R.E., *The 1953 Suva earthquake and tsunami*, Bull. Seismol. Soc. Amer., 52, 1–12, 1962.
- HSU, M.K., *Tsunamis in Taiwan and its near-by regions*, Acta Oceanogr. Taiwanica, 35, 1–16, 1996 (in Chinese).
- IRVING, E.M., and J.S. TEVES, *The Iloilo earthquake of January 25, 1948, Panay Island, P.I.*, Philippine Geologist, 2, (2), 6–17, 1948.
- KANAMORI, H., J.W. GIVEN, and T. LAY, *Analysis of body waves excited by the Mount St. Helens eruption of May 18, 1980*, J. Geophys. Res., 89, 1856–1866, 1984.
- KVALE, A., *Seismic seiches in Norway and England during the Assam earthquake of August 15, 1950*, Bull. Seismol. Soc. Amer., 45, 93–113, 1955.

- MA, K.-F., and M.-F. LEE, *Simulation of historical tsunamis in the Taiwan region*, TAO, 8, 13–30, 1997.
- MANSINHA, L., and D. E. SMYLIE, *The displacement fields of inclined faults*, Bull. Seismol. Soc. Amer., 61, 1433–1440, 1971.
- MASÓ, M.S., *Great earthquake and tidal wave in Southern Mindanao, P.I.*, Bull. Seismol. Soc. Amer., 8, 125–126, 1918.
- MEGAWATI, K., F. SHAW, K. SIEH, Z. HUANG, T.-R. WU, Y. LIN, S.K. TAN, and T.-C. PAN, *Tsunami hazard from the subduction megathrust of the South China Sea: Part I. Source characterization and the resulting tsunami*, J. Asian Earth Sci., 36, 13–20, 2009.
- MÜLLER, R.D., M. SDROLIAS, C. GAINA, and W.R. ROEST, *Age, spreading rates, and spreading asymmetry of the world's ocean crust*, Geochem. Geophys. Geosyst., 9, (4), Q04006, 19 pp., 2008.
- NANAYAMA, F., K. SATAKE, R. FURUKAWA, K. SHIMOKAWA, K. SHIGENO, and B.F. ATWATER, *Unusually large earthquakes inferred from tsunami deposits along the Kuril Trench*, Nature, 424, 660–663, 2003.
- NELSON, A.R., H.M. KELSEY, and R.C. WITTER, *Great earthquakes of variable magnitude at the Cascadia subduction zone*, Quatern. Res., 65, 354–365, 2006.
- OKAL, E.A., and C.E. SYNOLAKIS, *Far-field tsunami hazard from mega-thrust earthquakes in the Indian Ocean*, Geophys. J. Intl., 172, 995–1015, 2008.
- OKAL, E.A., and D. REYMOND, *The mechanism of the great Banda Sea earthquake of 01 February 1938: Applying the method of Preliminary Determination of Focal Mechanism to a historical event*, Earth Planet. Sci. Letts., 216, 1–15, 2003.
- OKAL, E.A., H.M. FRITZ, C.E. SYNOLAKIS, J.C. BORRERO, R. WEISS, P.J. LYNETT, V.V. TITOV, S. FOTEINIS, B.E. JAFFE, P.L.-F. LIU, and I. CHAN, *Field Survey of the Samoa Tsunami of 29 September 2009*, Seismol. Res. Letts., 81, 577–591, 2010.
- OKAL, E.A., J.C. BORRERO, and C.E. SYNOLAKIS, *Evaluation of tsunami risk from regional earthquakes at Pisco, Peru*, Bull. Seismol. Soc. Amer., 96, 1634–1648, 2006.
- OKAL, E.A., *Use of the mantle magnitude M_m for the reassessment of the seismic moment of historical earthquakes. I: Shallow events*, Pure Appl. Geophys., 139, 17–57, 1992.
- PELINSKY, E., D. YULIADI, G. PRASETYA, and R. HIDAYAT, *The 1996 Sulawesi tsunami*, Natural Hazards, 16, 29–38, 1997.
- REPETTI, W.C., *Catalogue of Philippine earthquakes, 1589–1899*, Bull. Seismol. Soc. Amer., 36, 133–322, 1946.
- REPETTI, W.C., *The China Sea earthquake of February 14th, 1934*, in: *Seismological Bulletin for 1934 January-June*, Dept. Agriculture & Commerce, Govt. of the Philippine Is., pp. 22–29, Manila, 1934.
- REYMOND, D., and E.A. OKAL, *Preliminary determination of focal mechanisms from the inversion of spectral amplitudes of mantle waves*, Phys. Earth Planet. Inter., 121, 249–271, 2000.
- ROMANOWICZ, B. and G. SUÁREZ, *An improved method to obtain the moment tensor of earthquakes from the amplitude spectrum of Rayleigh waves*, Bull. Seismol. Soc. Amer., 73, 1513–1526, 1983.
- SATAKE, K., K. SHIMAZAKI, Y. TSUJI, and K. UEDA, *Time and size of a giant earthquake in Cascadia inferred from Japanese tsunami records of January 1700*, Nature, 379, 246–249, 1996.
- SCHOUTEN, G., *Voyage de Gauthier Schouten aux Indes Orientales, commencé l'an 1658 et fini l'an 1665*, Vol. 1, pp. 322–323, Pierre Cailloué, Rouen, 1725.
- SELLA, G., T.F. DIXON, and A. MAO, *REVEL: A model for recent plate velocities from space geodesy*, J. Geophys. Res., 107, (B4), ETG_11, 32 pp., 2002.
- SOLOV'EV, S.L., and Ch.N. GO, *A catalogue of tsunamis on the Western shore of the Pacific Ocean*, Can. Transl. Fisheries Aquat. Sci., 5077, 439 pp., Ottawa, 1984.
- SOLOV'EV, S.L., Ch.N. GO, and Kh.S. KIM, 1986 *Katalog tsunamiv Tikhom Okeane, 1969–1982 gg.*, Akad. Nauk SSSR, 164 pp., 1986 (in Russian).
- STEWART, G.S., and S.N. COHN, *The 1976 August 16, Mindanao, Philippines, earthquake ($M_s = 7.8$)—evidence for a subduction zone South of Mindanao*, Geophys. J. Roy. astr. Soc., 57, 51–63, 1979.
- SYNOLAKIS, C.E., *Tsunami and seiche*, in: *Earthquake Engineering Handbook*, ed. by W.-F. Chen and C. Scawthon, pp. 9_1–9_90, CRC Press, Boca Raton, 2003.
- SYNOLAKIS, C.E., E.N. BERNARD, V.V. TITOV, U. KÂNOĞLU, and F.I. GONZÁLEZ, *Validation and verification of tsunami numerical models*, Pure Appl. Geophys., 165, 2197–2228, 2008.
- SYNOLAKIS, C.E., J.-P. BARDET, J.C. BORRERO, H.L. DAVIES, E.A. OKAL, E.A. SILVER, S. SWEET, and D.R. TAPPIN, *The slump origin of the 1998 Papua New Guinea tsunami*, Proc. Roy. Soc. (London), Ser. A, 458, 763–789, 2002.
- TITOV, V.V., and C.E. SYNOLAKIS, *Numerical modeling of tidal wave runup*, J. Waterw. Port, Coastal & Ocean Eng., 124, 157–171, 1998.
- TSUJI, Y., F. IMAMURA, H. MATSUTOMI, C.E. SYNOLAKIS, P.T. NANAG, JUMADI, S. HARADA, S.S. HAN, K. ARAI, and B. COOK, *Field survey of the East Java earthquake and tsunami of June 3, 1994*, Pure Appl. Geophys., 144, 839–854, 1995.
- VANNESTE, M., J. MIENERT, and S. BUNZ, *The Hinlopen slide: a giant submarine slope failure on the Northern Svalbard margin*, Arctic Ocean. Earth Planet. Sci., 245, 373–388, 2006.
- WALLACE, R.E., G. PARARAS-CARAYANNIS, R. VALENZUELA, and J.N. TAGGART, *Earthquake and tsunamis of August 16, 1976, Mindanao, Philippines*, Geol. Soc. Amer. Abst. Prog., 9, 523, 1977 (abstract).
- WESSEL, P., and W.H.F. SMITH, *Free software helps map and display data*, Eos, Trans. Amer. Un., 72, 441 and 445–446, 1991.
- WYSESSON, M.E., E.A. OKAL, and K.L. MILLER, *Intraplate seismicity of the Pacific Basin, 1913–1988*, Pure Appl. Geophys., 135, 261–359, 1991.
- YE, L., X. WANG, and C. BAO, *Tsunami in the China seas and its warning service*, Proc. IUGG/IOC Intl. Symposium, 23–27 Aug. 1993, pp. 771–778, 1993.
- ZACHARIASEN, J., K. SIEH, F.W. TAYLOR, R.L. EDWARDS, and W.S. HANTORO, 1999 *Submergence and uplift associated with the giant 1833 Sumatran subduction earthquake atoll: Evidence from coral microatolls*, J. Geophys. Res., 104, 895–919, 1999.
- ZHOU, Q., and W.M. ADAMS, *Tsunami risk analysis for China*, Natural Hazards, 1, 181–195, 1988.